Evaluation of Single Lead ECG Quality Based on Electrode Features and Positioning

Master of Science (tech.) Thesis
University of Turku
Department of Computing
2024
Milja Lempinen

Supervisors:
Matti Kaisti, PhD
Jukka-Pekka Sirkiä, M.Sc.

UNIVERSITY OF TURKU
Department of Computing

Milja Lempinen: Evaluation of Single Lead ECG Quality Based on Electrode Features and Positioning

Master of Science (tech.) Thesis, 50 p.
April 2024

Wearable devices for heart rate and ECG monitoring have been gaining popularity in the last two decades. The wearable market is still growing and looking into the quality and the reliability of the devices is ever so important. The aim of this thesis is to observe how reliable different setups of wearable, single lead ECG devices are, and how the electrodes and their placement affect the resulting signals.

The research questions were answered with literature review and laboratory experiments conducted for this thesis. In the experiments, a total of six different setups of three different single lead ECG signal collection devices were observed. The setups had differing electrode materials, distances, or sizes. The main interest points in the produced signals were the amplitudes and waveform quality. The results were evaluated with statistical methods, including visualisations of the signals.

The results and conclusions were, that altering the electrode material, distance, or size of the signal collection setup affects the resulting signal. The electrode material affects the signal quality the most, while the distance and the electrode size affect the average waveforms. The results presented in this thesis do not contradict any previous research on the same topic but do support their conclusions gathering the different alterations in the same reference framework.

Keywords: ECG, heart, monitoring, health technology, biosignals, wearables

UNIVERSITY OF TURKU
Department of Computing

Milja Lempinen: Evaluation of Single Lead ECG Quality Based on Electrode Features and Positioning

Master of Science (tech.) Thesis, 50 p.
April 2024

Puettavien sykemittareiden ja EKG-monitorien suosio on kasvanut viimeisen kahden vuosikymmenen aikana merkittävästi. Puettavien laitteiden markkina kasvaa yhä edelleen ja siksi onkin erityisen tärkeää selvittää näiden laitteiden tuottamien signaalien luotettavuuteen ja laatuun. Tämän diplomityön tavoitteena on tarkastella erilaisten yksikanavaisten laiteasetelmien luotettavuutta ja sitä, kuinka elektrodien materiaalit ja asettelu vaikuttavat signaaliin.

Tutkimuskysymyksiin haettiin vastauksia kirjallisuudesta ja työtä varten toteutettujen mittausten tuloksista. Näissä mittauksissa kerättiin dataa yhteensä kolmesta eri laitteesta ja kuudesta eri laiteasetelmasta. Laiteasetelmat erosivat toisistaan elektrodien materiaalin, etäisyyden, tai koon osalta. Pääasialliset tarkastelukohteet olivat signaalien amplitudit ja aaltomuotojen laatu. Mittausten tuloksia arvioitiin käyttämällä tilastollisia menetelmiä sekä visualisoimalla tuloksia.

Työn johtopäätöksenä on, että muutokset elektrodien materiaalissa, etäisyydessä, tai koossa vaikuttavat EKG-signaaliin. Eri laiteasetelmien tuottamat signaalit eroavat toisistaan osittain merkittävästikin. Elektrodien materiaali vaikuttaa erityisesti signaalin laatuun, kun taas etäisyys ja koko vaikuttavat aaltomuotoon. Työn tulokset tukevat aiempaa tutkimusnäyttöä, ja eri lähteistä nousseet tulokset ja asetelmat on koottu yhteen kokonaisuuteen yhdistettynä tässä työssä tehtyihin mittauksiin.

Keywords: ECG, heart, monitoring, health technology, biosignals, wearables

Contents

1 Introduction

Electrocardiography is a medical measuring technology that is used to observe the electrical activity of the heart (Eerola 2022). It is an invaluable diagnostic tool to identify, for example, arrhythhmias and infarcts (Mäkijärvi 2019a). The first applications of electrocardiography date back to the 19th century (Yang et al. 2015). Willem Einthoven presented the first successful method in the beginning of the 20th century. He was later awarded a Nobel prize in Medicine for his findings (AlGhatrif and Lindsay 2012). The basic principles have changed little during the decades, but newer trends, such as wearable devices, have gotten a stronger foothold (Yang et al. 2015).

In this thesis, the wearable, single lead devices are examined. These devices have great ambulatory possibilities, but also some limitations, such as reluctance among medical professionals to adopt these devices to broader use. (Santala 2022, Hilbel and Frey 2023). The use of wearable ECG devices is at the moment most popular among people interested in their personal fitness, but even medical use is growing (Piwek et al. 2016). For example, in the Finnish field of occupational healthcare, the use of wearable ECG devices to monitor the rhythm of the heart is growing in popularity (Rauttola et al. 2019).

The main research questions, that this thesis attempts to answer, are as follows:

1. Are the wearable single lead ECG a reliable method to measure ECG?
2. How much do the material, size, and distance of the electrodes affect the result of the measurement?

To answer these questions, a broad selection of literature was explored. Most of the material are from scientific publications, but also practical guides and medical training material has been used to better understand and describe the subject of electrocardiography and the functions of the human heart as these publications describe the state of the art in medicine.

In addition to the review of literature, experiments with three different single lead devices were conducted, because the literature did not give a comprehensive enough picture in regards of the chosen research questions. The results of the experiment are compared to the literature to complement the conclusions.

In the second chapter (Chapter 2), an overview on the subject is given. This includes the physical, electrical phenomena in the heart and how they appear in the visualisation of an electrocardiogram. Also the principles of wearable devices are introduced, as well as previous research on the subject.

In the third chapter (Chapter 3), the experiments are introduced and described. Additionally, the devices used are introduced and the conditions and subjects of the experiment are presented. The signal processing methods are described in this chapter as well.

In the fourth chapter (Chapter 4), the collected signals are analysed. The analysis results are then presented in the context of the previous research done.

2 Electrocardiography

2.1 Principal Concept

Electrocardiogram, or ECG, sometimes EKG, is a biosignal recording captured with an electrocardiography device measuring the electrical activity of the heart. It is used to observe the functions of the heart, as it contains information on the depolarisation and repolarisation of cardiac cells. (Thaler 2018c)

ECG is recorded from the surface of the skin, usually using wet electrodes. The electrodes are used for measuring changes in biopotential, the flow of ions. In the clinical setting, one of the most common types of electrodes used is the silver-silver chloride -electrode pairing (Ag/AgCl) (Lee and Kruse 2008). The Ag/AgCl electrodes have the best qualities in performace, while the dry electrodes have not been up to the clinical standards (Meziane et al. 2013). Studies show that the choice of electrodes affects the final resulting signal. For example, the sizing seems to impact the amplitudes, with larger electrodes producing lower amplitude signals (Nairn et al. 2020).

The history of modern ECG measured from the skin, dates back to the 19th century, when William Einthoven first recorded and described the process in his published work (Barold 2003). Since then, ECG has become a staple in the field of medicine

and especially cardiology. ECG is a completely safe, non-invasive procedure, making it the preferred method to screen the heart (Eerola 2022). In the 21st century, consumer electronic developers have taken an interest in bringing especially wearable, single-lead ECG devices to the market. For example brands, such as Apple and Samsung, have included ECG in their smartwatches.

2.2 ECG Leads

An understanding of the geometry of the heart is required to understand the directions of the electrical polarity of the heart as the electrodes on the skin have to be placed according to the direction of the electrical polarity. The heart should be observed as a three-dimensional entity, which is why reading its electrical activity from one direction only is not enough to get an understanding of the complex processes that happen during the cardiac cycle (Thaler 2018a). These directions are visualised in Einthoven's triangle shown in Figure 2.1. From the Eithoven's triangle, we can also read the current directions of the basic leads of ECG. (A. L. Goldberger, Z. D. Goldberger, and Shvilkin 2018b)

In the early 20th century ECG-solution, three limb leads were used. These are known as leads I, II and III, or Einthoven's limb leads. Lead I measures the potential difference between left arm and right arm. The potential difference is equal to potential measured in the RA electrode subtracted from the LA electrode (LA-RA). (A. L. Goldberger, Z. D. Goldberger, and Shvilkin 2018b)

Similarly to lead I, lead II is equal to the potential difference of right arm and left leg, or LL-RA. Lead III is again the potential difference between left leg and left arm, or LL-LA. (A. L. Goldberger, Z. D. Goldberger, and Shvilkin 2018b)

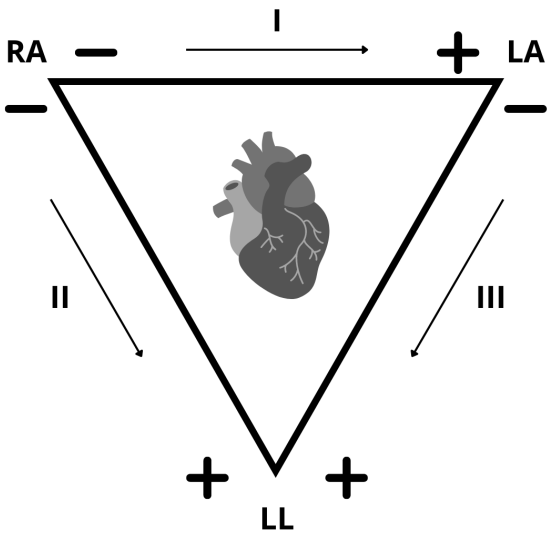

Figure 2.1: Einthoven's triangle visualised based on illustration in Goldberger's Clinical Electrocardiography (A. L. Goldberger, Z. D. Goldberger, and Shvilkin 2018b)

Adding to the three original leads, to better take into account the anatomy of the heart, three more leads were introduced in the 1930s. These are called the aVR, aVL, and aVF -leads, also known as the Goldberg leads. The *a* stands for augmented, V for voltage, and R, L, and F for right arm, left arm, and foot (left), respectively (Figure 2.2). The augmentation is based on two of the limb electrodes acting as a conjoined negative electrode, and one as the positive electrode. (Thaler 2018a)

Looking at the lead aVR, the right arm electrode is set as positive, while the left arm, and left leg electrodes are set as negative together. Similarly to aVL, left arm is positive and right arm and left leg together negative, and aVF has left leg as positive and right arm and left arm as negative. (Mäkijärvi and Korhonen 2019)

These augmented leads complement the Einthoven leads. This is especially visible, when looking at the geometry of the leads (Figure 2.2). This visualisation shows all of the leads and the augmented leads can be thought as vector sums of the original

three limb leads: for example, the aVR lead is the sum of the leads -I and -III. (A. L. Goldberger, Z. D. Goldberger, and Shvilkin 2018b)

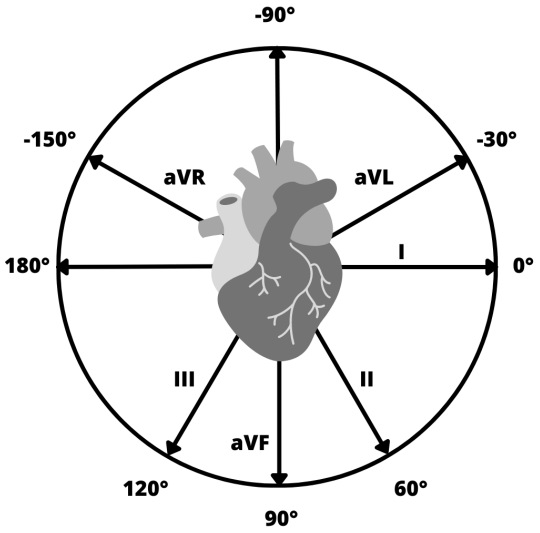

Figure 2.2: The geometry of the leads visualised. Illustration based on example in "The Only EKG Book You'll Ever Need"(Thaler 2018c)

The six limb leads are then again complemented with six precordial leads, or chest leads. These are numbered as V1, V2, V3, V4, V5, and V6. They are independent from the limb leads and help to obtain information regarding the functioning of the heart from the horizontal plane in addition to the vertical. The standard precordial leads are collected from six electrodes placed on the left side of the chest. (A. L. Goldberger, Z. D. Goldberger, and Shvilkin 2018b)

As the standard precordial leads are collected from the left side of the chest only, sometimes more information is needed, for example when the functioning of the right side is being observed. It is possible to complement the standard chest leads with their mirroring counterparts V1R to V6R. They are collected similarly to V1-V6, but from the right side of the chest. Leads collected from the backside are an option. They are numbered as V7, V8, and V9. These additional leads also describe the

potential changes in the horizontal plane and thus give information on the heart in the third dimension. (Thaler 2018a)

The leads can be assorted into four groups: anterior leads, left lateral leads, inferior leads, and right ventricular leads. These groups describe which section of the heart can be best observed by the leads. Anterior leads, V2, V3, and V4, describe the functioning of the heart from the front, while leads I, aVL, V5, and V6, or the left lateral leads, give more information on the functioning of the left side of the heart. The lower part of the heart can be best observed with the inferior leads, which are leads I, II, and aVF. The right ventricular leads are then left to give more focused information on the functioning of the right ventricle. (Thaler 2018c)

2.3 Waveform

ECG contains information on the phases of the cardiac cycle, displayed as the changes in the voltage measurable from, for example, the skin. The normal, lead II ECG waveform can be seen in Figure 2.3. As the leads are placed on the skin in differing angles in relation to the heart, the three-dimensionality of the heart causes the individual ECG leads to produce visually varying waveforms. They do, however, usually contain the same basic waves, even though the size and direction of those waves may differ between leads.

The cardiac cycle starts with the heart in the relaxed state. The first event of the cycle is the atrial depolarisation, which causes the *P-wave* in the ECG output. The P-wave is relatively small event and its shape describes the spread of depolarisation in the atria starting from the right and ending on the left atrium. (Thaler 2018b)

After the atrial depolarisation, there is a small break in the electric activity, caused

by the atrioventricular node's declined conductivity. After the electric signal passes through the AV-node, comes the ventricular depolarisation, which shows as the *QRS-complex* in the ECG (Thaler 2018b). The QRS compex has the greatest amplitude of any events in a normal ECG.

Repolarisation of the cardiac cells is the last phase of the cardiac cycle. This will show in the ECG as the *T-wave*, which has lower amplitude than the QRS-complex. The duration of the ventricular repolarisation is longer than other phases of the cardiac cycles, which makes the T-wave appear as a wider formation on the x-axis than other visible waves. (Korhonen and Mäkijärvi 2019)

An additional *U-wave* is sometimes visible. It can be observed immediately following the T-wave. When visible, the amplitude of the U-wave is very low. The origins of this wave are mostly unknown, but it is important to note the possibility of its existence as the main goal of this thesis is the quality analysis of ECG signals. (A. L. Goldberger, Z. D. Goldberger, and Shvilkin 2018a)

The amplitudes of the waves are highly dependant on the lead used. Certain leads have, for example, more prominent T-waves, like leads V2 or V3. The characteristics of the waveforms from the different leads of the standard 12-lead ECG are displayed in the table below (Table 2.1).

The different directions of the waves depending on the lead derive from the anatomy of the heart. As, for example, the P-wave marks the atrial depolarisation, it is more prominent on the leads that measure the vectors in direction of right atrium to the left ventricle. The biphasic wave is produced by leads measuring the potential difference in the direction of left atrium to right ventricle and the negative wave by

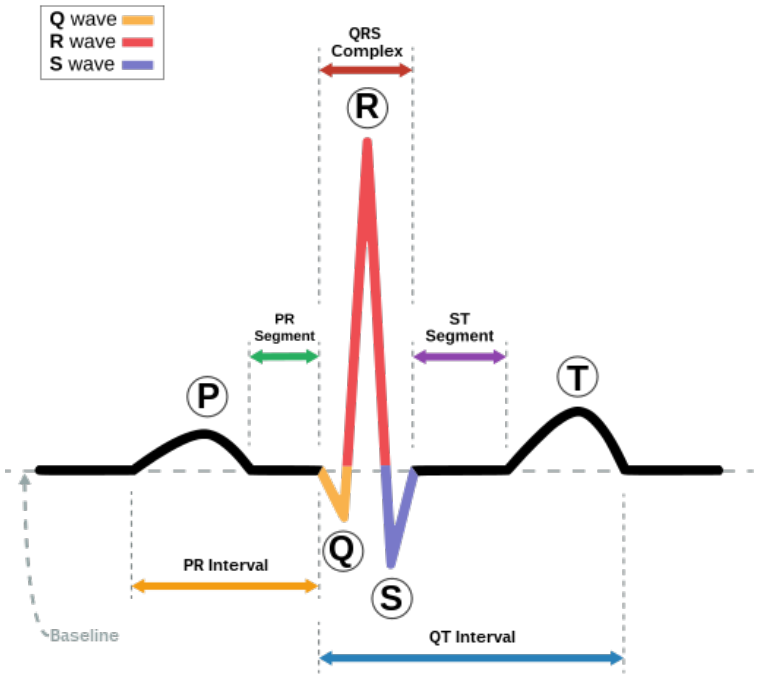

Figure 2.3: ECG normal waveform with different phases and peaks highlighted. (Wikimedia 2007)

leads in the direction of left ventricle to right ventricle. Similarly to the differences in P-waves, the visibility and direction of the other waves can be explained with the vector diagram of the leads. (Thaler 2018b)

The standard placement of the limb lead electrodes are on the limb extremites. However, a modification called Mason-Likar was introduced in 1966, where the electrodes are placed on the torso instead of the limb extremities (Mason and Likar 1966). The effects of this modification on the amplitudes of the signals depend on the lead. According to Rautaharju (et al.), the R peak amplitude of lead I is lower with the modified lead placement, while on the other hand grows in the lead II (Rautaharju et al. 1980). The placement of the limb electrodes is visualised in figure 2.4 below.

Lead	P-wave	Q-wave	R-peak	S-wave	T-wave
I	Positive	Negative	Positive	Not always visible	Positive
II	Positive	Not visible	Positive	Not always visible	Positive
III	Biphasic	Not visible	Positive	Negative	Positive
aVR	Negative	Not visible	Not visible	Negative (deepest)	Negative
aVL	Positive	Negative	Positive	Negative	Positive
aVF	Positive	Not visible	Positive	Negative	Positive
V1	Biphasic	Not visible	Positive (smallest)	Negative	Negative
V2	Varies	Not visible	Positive	Negative	Positive
V3	Varies	Negative	Positive	Negative	Positive
V4	Varies	Negative	Positive	Negative	Positive
V5	Varies	Negative	Positive	Negative	Positive
V6	Positive	Negative	Positive	Not always visible	Positive

Table 2.1: The directions of the different waves in the PQRST waveform in the basic 12-leads (Thaler 2018b).

2.4 As a Diagnostic Tool

ECG is primarily a diagnostic tool. It can be used in clinical settings to evaluate the health of the heart. Its non-invasive nature and ambulatory possibilities make it an invaluable option in diagnostics. (Mäkijärvi 2019a)

When reading the ECG, two things are observed: the sequence and order of the different waves of the ECG, and the waveform of the signal (Raatikainen, Mäkijärvi, and Parikka 2019a). In the Finnish teaching material for medical professionals, the recommended screening order is to first identify the overall waveform of the ECG, after which one should observe if the ventricular rate is abnormal in any way, and

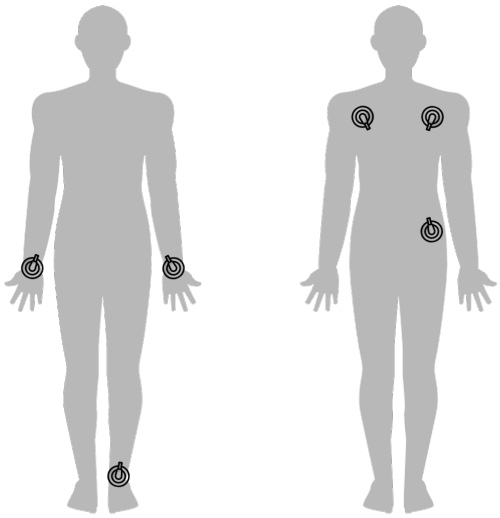

Figure 2.4: ECG limb lead electrode placement visualised. On the left, the standard placement and on the right the Mason-Likar modification.

then focus on the individual waves (Raatikainen, Mäkijärvi, and Parikka 2019b).

Different ECG abnormalities point to different diagnosis. One of the most common cardiovascular disease is the coronary artery disease (CAD), which can sometimes be diagnosed from the electrocardiogram. The abnormalities that can point to CAD include, but are not limited to, ST elevation in all leads, tall and peaked T-waves, and inverted T-waves in precordial leads. In addition, negative U-waves related to CAD can sometimes be observed. (Birnbaum, Wilson, and Nikus 2015)

Another important use case is the diagnosis of atrial fibrillation (AF). This is the most common type of arrythmia, that in Finland requires treatment (Duodecim 2021). From the ECG, it can be diagnosed based on abnormal heart rate, the absence of P-waves, and narrow QRS-complexes (Duodecim 2021).

There are multiple computational applications available for AF diagnosis. For example, Runnan He (et al.) suggest a solution based on convolutional neural net-

works, that performed with 99.23% accuracy in their testing with 25 ECG recordings (He et al. 2018). Consensus with the medical professionals today, however, is that these computational diagnostic tools cannot yet be trusted. In Finland, the official treatment guidelines recommend to manually check the ECG output in every case (Raatikainen and Parikka 2017). In the clinical setting, all medical devices are controlled. In Finland, the base of the regulations is the legislation on medical devices as well as directives of the European Union (Laki lääkinnällisistä laitteista, 2021/719).

When used in acute situations, for example in an ambulance, the personnel will take ECG with 12 leads. This is the diagnostic standard. Depending on the symptoms, even 14 leads can be considered. These devices are portable for easy transportation. They print out the electrocardiogram on a piece of paper. In Finland, the standard writing speed is 50 mm/s for all clinical ECG (Mäkijärvi 2019b).

There are also ambulatory ECG solutions available, that can be used either for extended periods of time or when needed (Steinberg et al. 2017). These devices have one or multiple leads and are used to screen for asymptomatic heart conditions or for continuous monitoring of an existing condition (Nault et al. 2019). The standard for ambulatory ECG is a three-lead "Holter", which is named after the developer, N. J. Holter (J. Adamec and R. Adamec 2008).

Another special use case for the electrocardiography is a cardiac stress test. The test is usually conducted with a 12-lead ECG device with changes in electrode placement according to Mason-Likar modifications (Laukkanen and Nieminen 2016). The cardiac stress test is used to screen for symptoms that present themselves in stress, which means that the ECG is taken in motion, either on a treadmill or a bike. The movement during the measurements affect the signal and is usually mitigated by filtering. The possible sources of noise are, for example, powerline contamination,

electromyographic noise, and high frequency noise (Bortolan et al. 2015).

2.5 Wearable ECG Devices

There are multiple options of wearable ECG devices on the market. Already in 2016 in the United States of America, 15% of consumers reported to use some kind of wearable health monitor continuously (Piwek et al. 2016). In 2023, a survey by Statista reported that 32% of the consumers used a wearable device (Statista 2024). In a review by the Finnish Institute of Occupational Health, it is stated that most often wearables are used to track the heart rate or heart rate variability in the context of occupational health (Rauttola et al. 2019). The main group of consumers for health monitoring wearables is likely to be already healthy adults, who want to track their performance in, for example, sports (Piwek et al. 2016).

In sports, a belt style ECG based heart rate monitor is a traditional choice. These kinds of ECG devices can be made of, for example, stretchy synthetic material with electrodes made from plastic polymers with conductive capabilities. Neither of the two of the best known commercial Finnish founded brands, Polar and Suunto, declare the electrode material of their heart rate belts (P. E. Oy 2020, S. Oy 2020). In the picture below, the material of the electrodes of Suunto's heart rate belt can be seen (Figure 2.5). The electrodes are harder than the other parts of the belt and located on both sides of the sternum when worn. This belt is commercially available.

For longer ECG measurement periods, one option for a wearable solution is a monitoring patch. A patch is applied on the skin with an adhesive and the electrodes being in close proximity of each other. With these types of devices, it is possible to

Figure 2.5: Suunto heart rate belt's electrodes photographed. No material information was available for this product.

monitor the heart for up to 14 days (Lobodzinski 2013). They have been shown to facilitate the diagnosis of atrial fibrillation (Steinhubl et al. 2018).

Furthermore, research on different textile based wearables has been conducted. For example, Nigusse (et al.) suggest that textile based electrodes could be better suited for long term use than traditional wet electrodes (Nigusse et al. 2021). The textile electrodes can be made of, for example, silver or titanium coated fibers (An and Stylios 2018, Fontana et al. 2019).

One example of a popular wearable ECG device is the Apple Watch. It is a smartwatch designed and manufactured by one of the most recognisable brands worldwide in 2020 (Swant 2020). Apple also claimed to be the first manufacturer to offer ECG on their smartwatch-product. The FDA in the United States of America has approved Apple's technology to recognise atrial fibrillation as a medical device. They state that the formed circuit creates an "ECG waveform similar to a Lead I" but they do not claim it to be equal. The smartwatch's ECG and the reading software

is claimed to have 98 percent sensitivity for atrial fibrillation events. (*Using Apple Watch for Arrhythmia Detection* 2020)

2.6 Previous Research on Single Lead ECG

The basic research of the ECG electrode placement was done in the first half of the 20th century. For example, Charles E. Kossman, MD, and Franklin D. Johnston, MD, conducted a study with 30 male participants on adding the precordial leads to the then standard six leads in 1935 (Kossmann and Johnston 1935). This study explores how the different waves relate to each other when the electrodes are placed on the precordium instead of the limbs. This information lays ground for the adaptations of the precordial leads in the years after.

Atrial fibrillation diagnostics is one of the practical applications for wearable devices. For example, Onni Elmeri Santala's doctoral dissertation on wearable ECG devices and the reliability of the AF detection from the signals they produce explores these possibilites (Santala 2022). The dissertation presents three studies on these devices, first one being conducted with a single lead necklace ECG device and the two others with an ECG patch and a heart rate belt. All of the devices listed in the dissertation are similar to the ones that were used in the experiment conducted for this thesis. The conclusion of Santala's research is that the quality of the signals produced by all of the devices are good enough to be used for AF diagnostics.

More types of arrythmias were included in a clinical study by Haverkamp, Fosse and Schuster, which focused on specific applications that would take single lead ECG as input (Haverkamp, Fosse, and Schuster 2019). According to their findings, a software called ECG Check by a company Cardiac Designs can identify multiple types of

arrythmia with "acceptable sensitivities and specificities" (Haverkamp, Fosse, and Schuster 2019). This study is limited to a specific software, but it does contribute to the conclusion that arrythmias are possible to diagnose automatically from a single lead.

Furthermore, Thomas Hilbel and Norbert Frey explored the advantages and disadvantages of consumer electronics ECG devices in 2023 (Hilbel and Frey 2023). Their conclusions support the previous ones, as they also found that the diagnostics of AF can highly benefit from the wearable, single lead ECG devices being easily available. However, they also highlight the limitations of these devices and state, that ischemia as well as myocardial infarctions are not recognisable from any of the signals from the single lead devices.

3 Methods

For this thesis, a laboratory experiment was planned and executed. The end goal of this experiment was to collect ECG-signal data from wearable devices and compare the collected data to a reference signal. The comparison was done to analyse the quality of the signals and evaluate their potential to be used in diagnostic settings.

3.1 Devices

Three observable devices were used in the experiments. All observable devices are based on the same sensor, Movesense Sensor. This sensor is not officially approved for medical use (Movesense 2023c). The sensor was connected to different kinds of electrodes.

Device number one is a two-electrode patch-type entity (Figure 3.1). This was built for research purposes by 3D-printing a shell for the Movesense sensor and connecting two cords for the electrodes to the sensor. The electrodes used with this device were two different size Ambu BlueSensor Ag/AgCl -electrodes (Ambu 2021a, Ambu 2021b). These are medical grade electrodes that can be used in ambulatory ECG for short periods.

The second device is a necklace ECG-sensor (Figure 3.2). It is an experimental ECG recording device based on the same Movesense sensor as the patch. It is set in a 3D-printed, flat, oval-shaped shell, that has two electrodes attached to it on both sides. The electrodes of the necklace are made of silver and they are meant to be used dry.

The third observable device is a heart-rate belt by Suunto. The Movesense sensor attaches to the middle of the belt, made from flexible textile material. The electrodes are visible on the surface of the textile belt. No further information on the material is available. The recommendation is to slightly wet the electrodes before use, but this was not done in the experiments due to the belt being responsive without this step as well.

As a reference, GE's patient monitor was used. The monitor was only able to give out one lead at a time, when three electrodes were connected, which leads to limitations in the analysis phase. This monitor is a medical device.

The sampling rate of the observable devices is 128 Hz. This was chosen, as it resembles the typical use of these types of sensors. In the reference device, the sampling rate is 100 Hz. This is the minimum sampling rate that was available for the device.

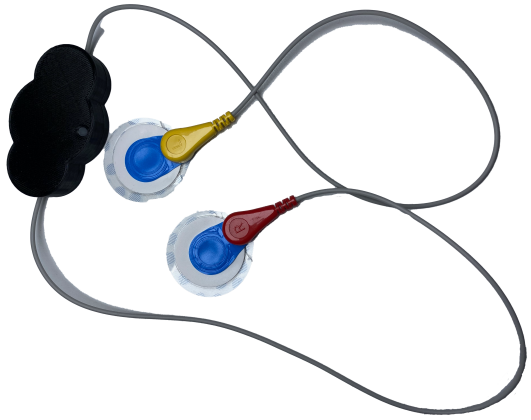

Figure 3.1: The loose-cord setup mimicking a patch type measurement device photographed. Red clip is for right side and yellow clip for left side.

Figure 3.2: The necklace measurement device photographed from both sides.

3.2 Measurements

The measurements of observable devices were taken simultaneously with the reference ECG, one device at a time. In total six setups were observed: first setup was the patch with cords with electrode size of 40 mm and distance of 5 cm, second setup was the patch with cords with electrode size of 56 mm and distance of 5 cm, third setup was the patch with cords with electrode size of 40 mm and distance of 15 cm, fourth setup was the patch with cords with electrode size of 40 mm and distance of 30 cm, fifth setup was the necklace, and the sixth setup was the HR belt. The positioning of the electrodes for the patch-setups can be seen below in

Figure 3.3, the placement of the hear rate belt and the necklace device in Figure 3.4. These setups were chosen to compare how the placement, size, and material of the electrodes affect the signal.

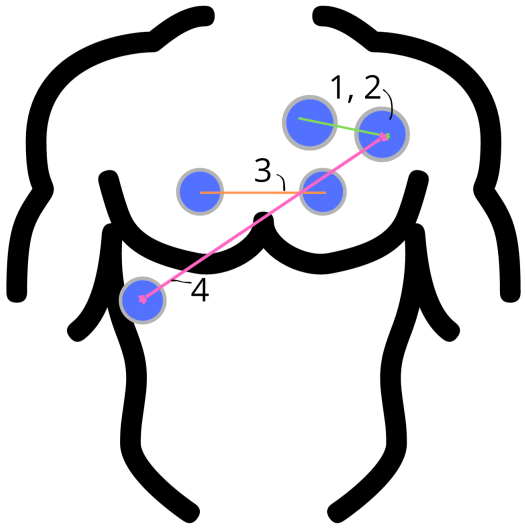

Figure 3.3: Positioning of the electrodes of the patch-like device in the experiment. Numbers indicate the setups.

The first step was to place and adjust the devices. The subject was given clear instructions on how to place the electrodes of the 3-electrode ECG, the patch, and the belt. After this, the placements and contact of the electrodes was verified. The subject was also given the necklace. All measurements were taken in resting state. The subject was instructed to lay down as relaxed as possible and the devices were switched on simultaneously. Two (2) 1-minute measurements were taken for each device individually rotating the device in use in following order:

1. patch with cords with electrode size of 40 mm and distance of c. 5 cm, reference

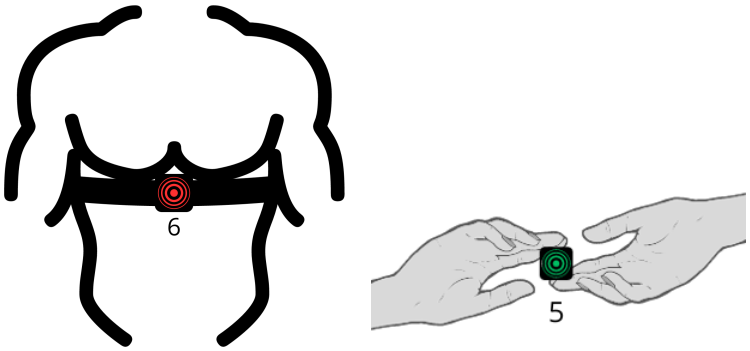

Figure 3.4: Positioning of the hr-belt (6) and necklace (5) devices.

measurement with patient monitor's lead I

2. patch with cords with electrode size of 56 mm and distance of c. 5 cm, reference measurement with patient monitor's lead I

3. patch with cords with electrode size of 40 mm and distance of c. 15 cm, reference measurement with patient monitor's lead I

4. patch with cords with electrode size of 40 mm and distance of c. 30 cm, reference measurement with patient monitor's lead I

5. EKG necklace, reference measurement with patient monitor's lead I

6. HR belt, reference measurement with patient monitor's lead I

The rotation was repeated twice. In total this led to 12 measurements per subject. The reserved time for each participant was 30 minutes.

In total, the measurements were taken from seven volunteers. All seven participants were females between ages 18 and 25. This makes for a homogeneous test group.

The mean age of the participants was 22.4 years and the standard deviation (SD) 2.9 years. Two reported having sometimes experienced arrhythmia. No further health information was collected from the participants.

The measurements took place in the facilities of University of Turku. All measurements were taken during the same day using the same devices on each participant. In total, over 84 minutes of ECG data from the observable devices was collected.

The facilities were not completely disturbance-free. Electrical devices, such as laptops, mobile phones, and fluorescent lamps, were present in the room and had potential to cause noise in the collected signals. To minimize the effect of these factors on the final signal, the signals were filtered in the processing phase.

Other possible causes of noise and disturbance are movements of the subjects and malfunctions of the devices. The reference device malfunctioned in four measurements, that were discarded.

3.3 Processing of the Collected Signals

The reference signals were collected using a device and software by GE. The software writes the signal into processable format. The timestamps are in Unix time format and the signal is in millivolts. The observable signals were collected using a mobile application built to record data from the Movesense-sensors. The timestamps are in the Unix time format, similarly to the reference device. The ECG channel has a default gain of 20V/V. The raw ADC readings were converted into millivolts using the following equation $ECGmv = 1000 * ADCcount/(2^{17} * Gain)$.

All signals were processed the same way before analysis. Preprocessing included

filtering and resampling of signals. The reference signal was resampled from 100 Hz to 400 Hz and the observable signal was resampled from 128 Hz to 400 Hz. This helps to better compare the signals in the time domain. Resampling was done using the Python library "Scipy's" signal processing module "Signal's" resampling function "resample" (SciPy 2023a). The resampling was done before filtering.

The filtering was done using a Butterworth filter built with the Scipy's Signal - module function "butter". The filter was set to be a 4th order bandpass filter with lowcut frequency of 0.5 Hz and highcut frequency of 45 Hz using the output of "second-order sections". The filter was applied to both the original and the resampled signals with the Scipy Signal method "sosfiltfilt" (SciPy 2023b). This method applies the filter both forward and backward to the signal thus making it zero phase. In the figure below, both an example of unfiltered and filtered and resampled signal can be seen (Figure 3.5). The main difference in the time domain visualisation is the higher sampling rate, as the original signals from the Movesense sensors were pre-filtered already on the recording phase, thus giving a relatively clean output without any additional filters (Movesense 2023a).

The difference between the unfiltered and filtered signals is best visible in the visualisation of the frequency domains (Figure 3.6). In the unfiltered signal, the signal power is distributed widely between frequencies 0 and 30, while in the filtered signal, the signal power is more concentrated on the lower end of the spectrum. The power spectral density (PSD) was calculated with Scipy Signal method "welch" (SciPy 2023c).

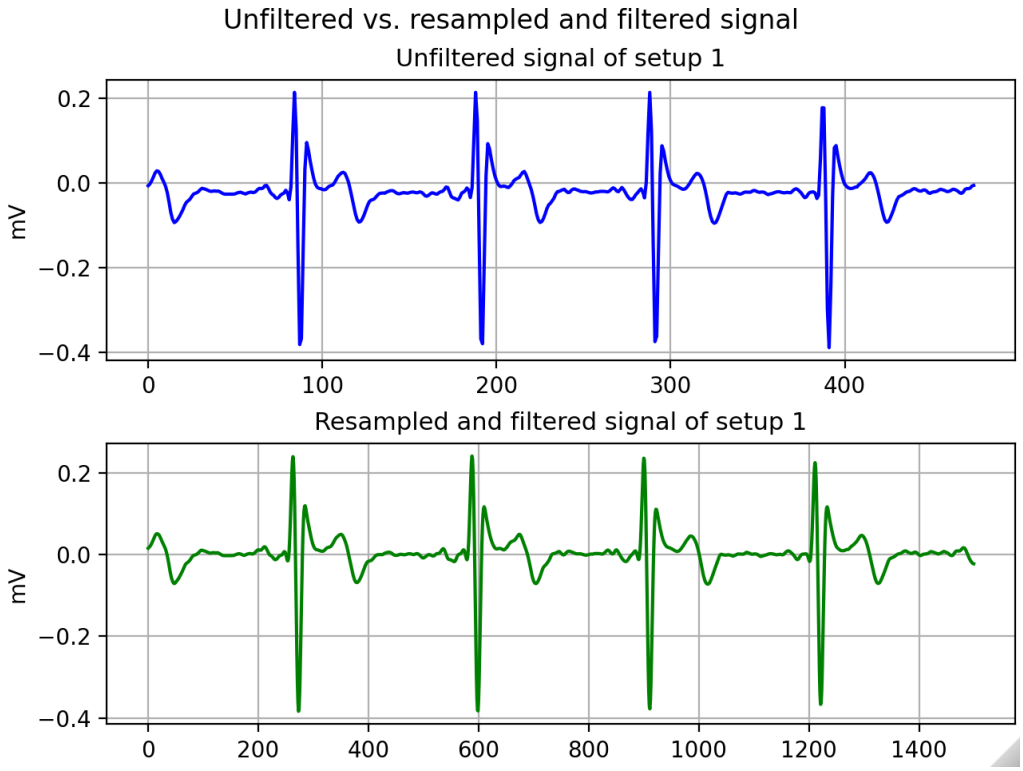

Figure 3.5: An example of a filtered and resampled signal with unfiltered signal.

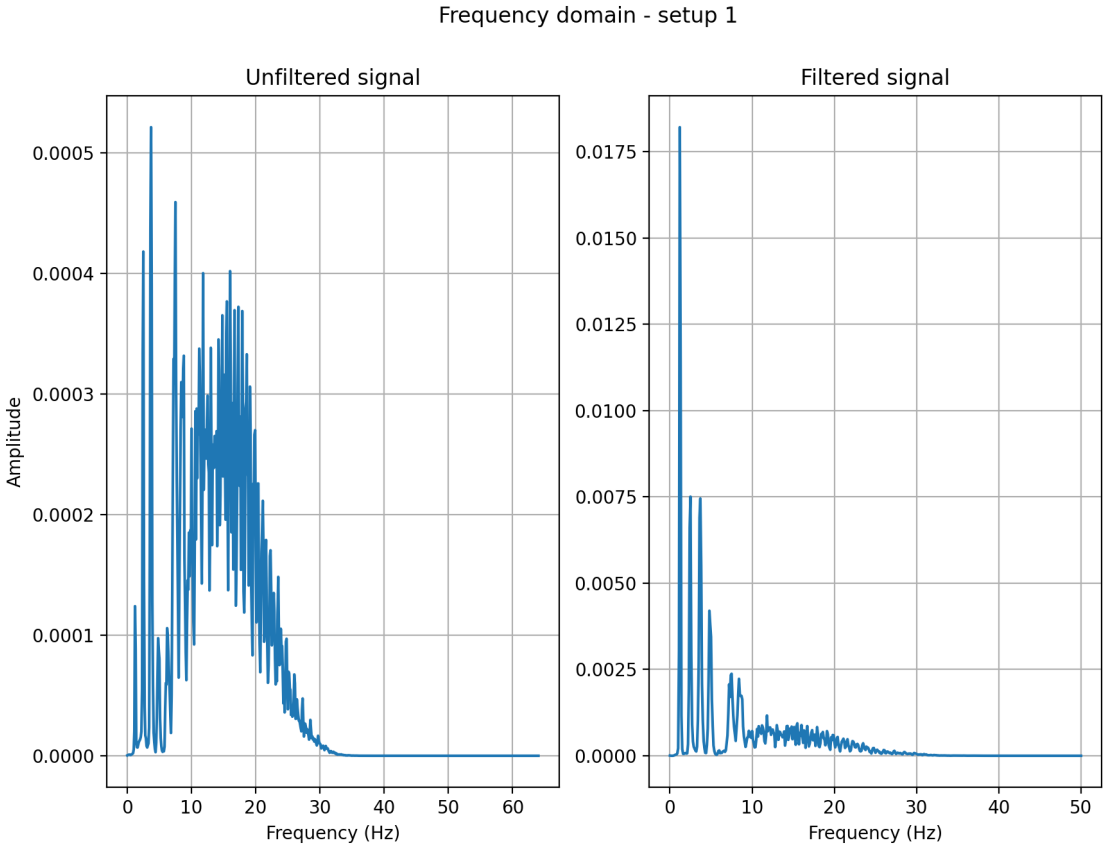

Figure 3.6: An example of a frequency domain of a filtered and resampled signal in comparison with the frequency domain of an unfiltered signal

4 Results and Discussion

4.1 Analysis Results

4.1.1 Quality Analysis of the Signals

Before the comparison and waveform analysis, the quality of the signals needs to be verified. The measurements were not taken in perfect conditions, so there are likely to be differences in quality between measurements and subjects.

First, all of the filtered signals were plotted to see whether they truly resembled an ECG signal. This step was to remove any signals that for any reason were extremely distorted. In some cases, the signals were so noisy that they could not be used. Eight signals were eliminated in this process.

Second step of quality assurance was to see whether the Movesense sensors had lost any data. According to their documentation and best practices, it is important to perform this kind of "sanity check" (Movesense 2023b). This was done by plotting the timestamp differences of each Movesense measurement. Five problematic signals were found and eliminated from the final dataset this way. In total, 4.8% of the reference signals and 7.1% of the observable signals were rejected. Some of the

signals were not perfect, but in this case those were included in the final dataset, since they were not deemed completely unusable either. The number of discarded signals by setup are displayed in table 4.1.

Table 4.1: Discarded signals by device.

Setup	Number of discarded signals
40 mm electrode, 5 cm dist.	2
56 mm electrode, 5 cm dist.	2
40 mm electrode, 15 cm dist.	0
40 mm electrode, 30 cm dist	1
Necklace	3
HR-belt	2
Reference	4

To further inspect the signal quality, all of the waveforms of each signal were extracted and compared to the mean of the waveforms to calculate a Pearson's correlation coefficient (PCC). This correlation coefficient showcases how uniform the signals' PQRST-waveforms are. In the table below, there are listed the average PCC for each measurement setup and their reference (Table 4.2)

In terms of waveform uniformity, it seems that the DUT waveforms have better correlation than the reference device's waveforms. This can be due to multiple factors, one being the differences in filtering as the signals produced by the DUTs were filtered twice: first with the built-in filter of the device and then again before

Table 4.2: Average Pearson correlation coefficients of PQRST-waveforms.

Setup	Average PCC of DUT	Average PCC of Reference
40 mm electrode, 5 cm dist.	0.9631	0.9150
56 mm electrode, 5 cm dist.	0.9793	0.9562
40 mm electrode, 15 cm dist.	0.9943	0.9660
40 mm electrode, 30 cm dist	0.9963	0.9659
Necklace	0.8064	0.9560
HR-belt	0.9559	0.9515

any analytics. The correlation seems to be similar between different setups for both reference device and DUTs. The only exception to this is setup 5, which is the necklace setup. Most likely this difference is due to the necklace setup being sensitive to movement artefacts. The highest correlation coefficents are found in setups with 15 cm distance and 30 cm distance. Both of these setups have electrodes located on both sides of the heart in the front.

In conclusion, the waveform quality of the observable devices, when looking at the consistency, is even greater that that of the reference device. It is thus possible to trust the devices other than the necklace to provide a signal of even quality.

4.1.2 Waveform Analysis

To analyse the average waveform of collected signals, four measures were chosen: the average R peak amplitude, the existence of the P wave, the maximal amplitude of the average T wave, and the width, or duration, of the QRS complex. The amplitudes of both R and T waves were calculated using an algorithm, while the P wave and QRS complex observations were made from the visualisation of the signal averages.

The QRS-complex's duration was measured manually. This was selected as the best approach, as implementing an automatic algorithm was deemed to be unreliable. The QRS-complex's form in the reference signal has great variation between subjects but only little variation between different setups with the same person. These observations were expected, as the measurements were all taken with same electrodes and in resting state. This implies that the reference device produces consistent signals. Only four subjects' data was used in this comparison, as some signals did not have clear enough Q or S -waves. An example of a waveform from which the QRS duration was not possible to measure can be seen in the figure 4.1. All measurements in this set were very similar, when it comes to the average waveform of the reference signal.

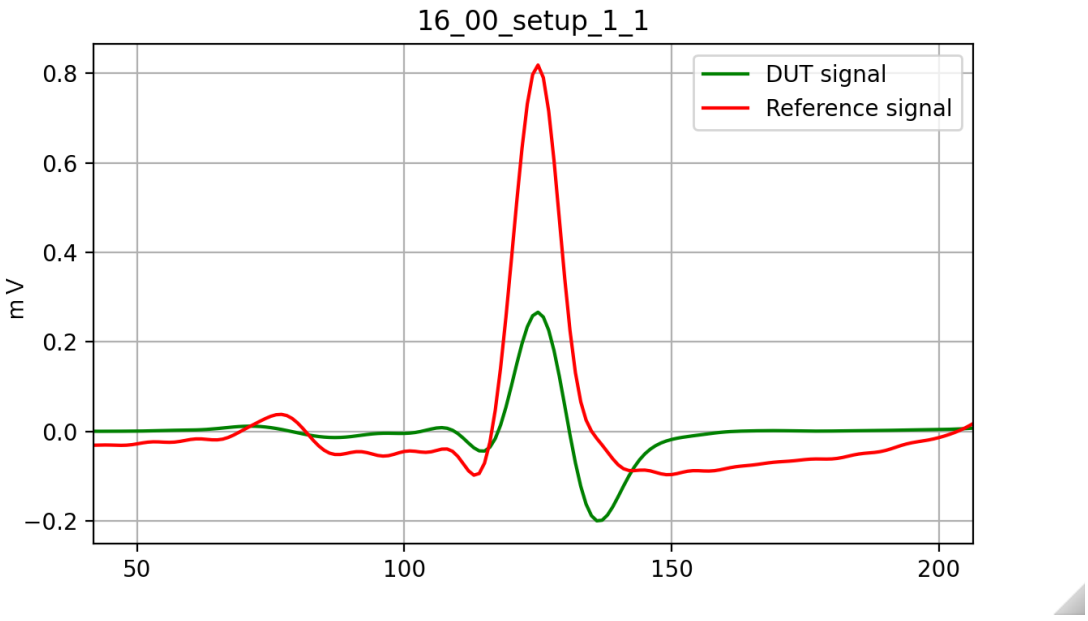

Figure 4.1: Average waveforms' QRS complexes of reference signal and DUT (patch setup 1) signal plotted in the same grid. Reference signal's S-wave's endpoint extremely difficult to detect.

For those signals that were able to be reviewed, the average QRS-complex's duration

is consistently longer in the DUT signals. The difference is for the most part between 2 and 10 milliseconds. In the following figure (Figure 4.2), it can be visually verified how the QRS complex is slightly wider in the average waveform calculated from the observable signal.

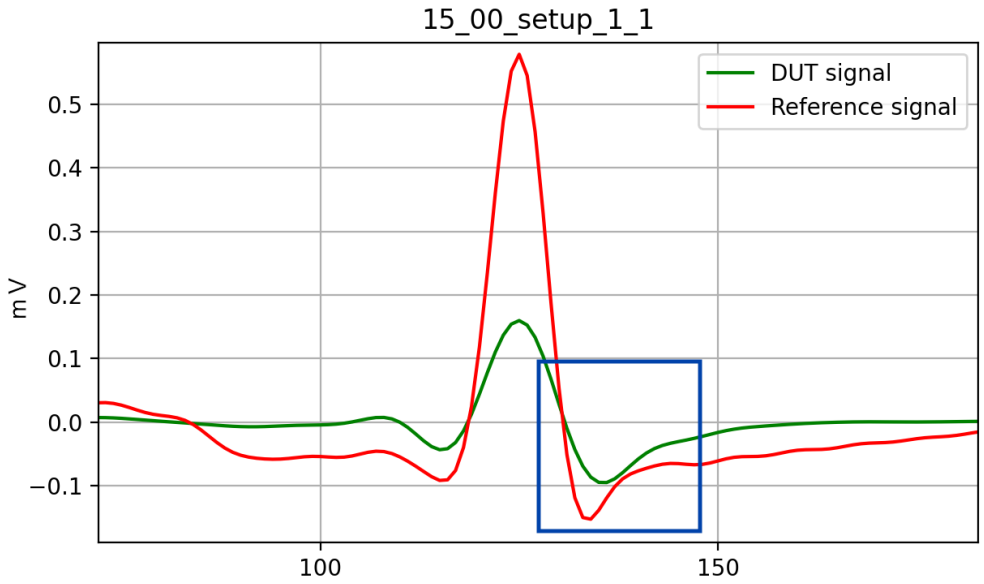

Figure 4.2: QRS complexes of the average waveforms of both reference and and DUT (patch setup 1) signals plotted in the same grid.

The differences in this example are subtle, yet noticeable. Even computational methods tested were able to detect the difference between Q and S waves' placement in relation to the R peak. In figure (4.2), we can observe that the DUT's average waveform, the waves are less steep in comparison to the reference. All of the measured QRS complexes were in the range of normal width, which is between 70 and 100 ms (Nikus, Aro, and Mäkijärvi 2016).

Simultaneously with the QRS measurements, the other peaks of the signals were manually inspected. A detection algorithm was used, but it did not work perfectly

on every case. The algorithm was based on the location of the R peak and the relation of the other waves to this center.

In most cases, the computational method did detect the peaks correctly. However, it did give multiple false positives. For example, in many cases, the algorithm found a P wave that most likely should be categorised as noise in the waveform. When visually verified, the P wave was present in almost every average waveform but in different place than the algorithm would suggest.

The wave was missing only in cases, where the average waveform could not be calculated due to inconsistencies in the signal. In figure 4.3, we can see how the P wave was not detected, but is still visible to the human eye (Figure 4.3).

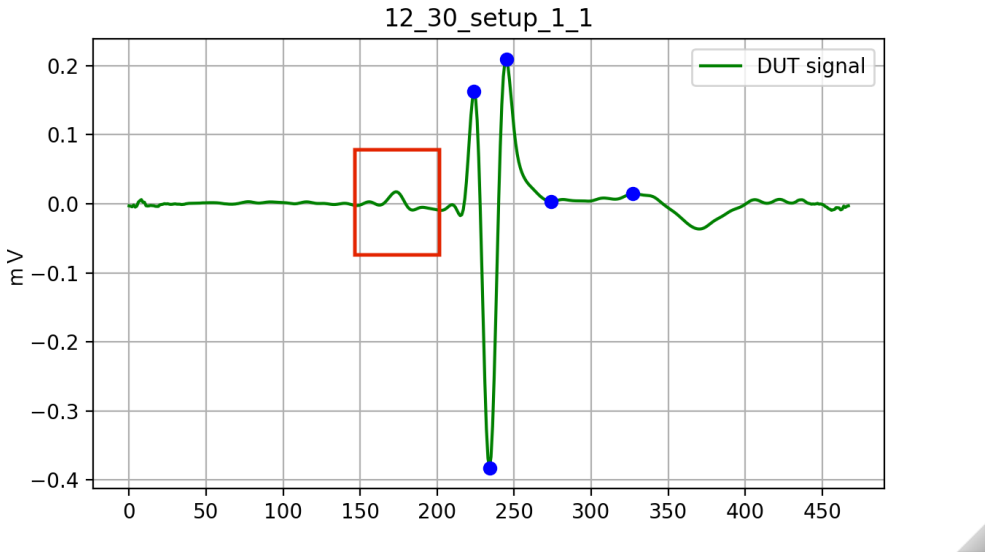

Figure 4.3: Average waveform calculated from the necklace's signal. P wave highlited with a red box.

Similarly to detecting the P wave, also T wave was in most cases correctly indentified by the algorithm. The T wave was not consistently missing in any other setups, except for the necklace. This is most likely due to the overall poor quality of the signals of the setup. The height of the wave differs a lot between the different setups.

Some of the T waves look like they would be almost inverted, but when compared to average location of the T wave in the reference signal, it seems that the inversion happens right after the wave. Inverted T waves are characteristic for leads aVR and V1. One example of this kind of behaviour of the signal can be seen in figure 4.4.

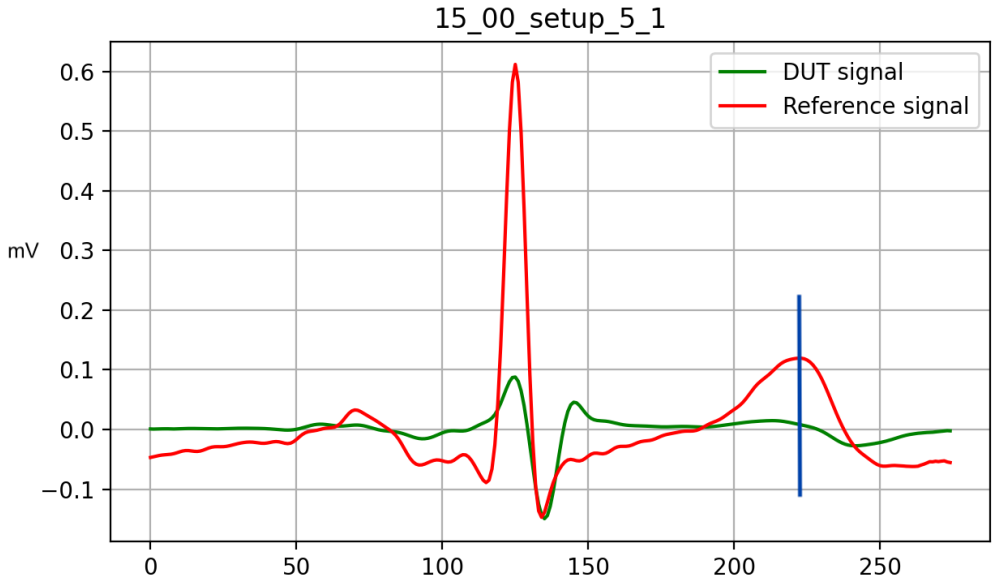

Figure 4.4: Average waveform calculated from the necklace's signal. T wave highlighted with a blue vertical line.

The highest average amplitude of the T wave was observed in the setup 4, which is the chest-to-side setup. This waveform does not resemble the waveform of lead I. Based on the electrode locations, it should be closer to lead -aVL. The second highest average amplitude was in the setup 3, with electrode placement closest to lead V1 or I. In other words, these signals should portray the electric current in the direction from left to right. The lowest average of the T wave amplitude was observed in the necklace setup, which should be closest to lead I, as it is taken from the right arm, or right index finger, to the left arm, or left index finger. This observation is possibly affected by the quality of the signals of the necklace setup,

as the T wave was either missing or miscalculated in multiple measurements. If the necklace is left out, the lowest average amplitude for T wave can be observed in the setup 2, which is the left chest setup with larger electrodes.

In almost all of the measurements, each individual wave was observable. This would imply that monitoring the rhythm should be possible with these setups, as the different waves point to different phases of the cardiac cycle (Korhonen and Mäkijärvi 2019).

4.1.3 Comparison of the Different Setups

To evaluate how the changes in the setups affect the resulting signal, the differences in the above listed key elements between the sets need to be assessed. As the goal is to look for the effect of distance and size of the electrodes, as well as the electrode material, following sets will give insight to these features:

1. Electrode size: setups 1 and 2 with wet electrodes of different sizes.
2. Electrode distance: setups 1, 3, and 4 with wet electrodes.
3. Electrode material: setups 4, 5 and 6 with Ag/AgCl, silver, and polymer electrodes, respectively.

First looking into the electrode size, the setups 1 and 2 have same or nearly the same electrode distance and placement, but different sized electrodes. In setup 1, a 40 mm electrode was used, while in setup 2 a 56 mm electrode was used. All of the key values seem to be quite close to each other. Setup 1 has slightly higher R peaks, with average of 0.19 mV, while setup 2 has R peak average amplitude of 0.15 mV. This difference in visual format is not striking, as can be seen in figure 4.5. The distance

of electrodes was measured from the centre, meaning that the effective distance of the 56 mm electrode setup was slightly smaller than of the 40 mm electrode setup. This might further negatively affect the amplitudes of the peaks.

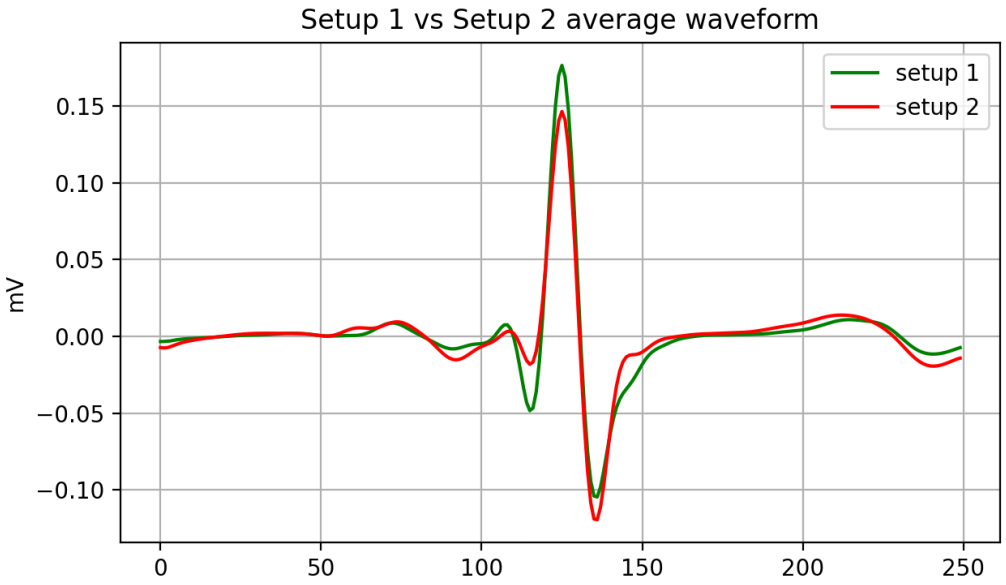

Figure 4.5: Visualisation of average waveforms of signals produced by setups 1 and 2. Both signals collected from the same subject.

Similarly to the R peaks, also T waves look alike. The highest point for both setups is around 0.03 mV. The P waves are also of similar heights. When looking at the two waveforms at the same time (Figure 4.5), it is visible that the 40 mm electrode setup has even deeper Q waves. On the other hand, the larger electrode setup produces cleaner looking S wave averages. The QRS complexes of both signals seem to be of almost equal length. As the visualisation shows, the average waveform of the 56 mm electrode setup is more sharp, while the respective graph from the smaller electrode setup has deeper Q wave and higher S peak (Table 4.3).

In the boxplot visualisation in the Figure 4.6, it is visible that most of the R peaks

Table 4.3: Average amplitudes and standard deviations (SD) of R and T waves in setups 1 and 2.

Wave		R peak	T wave max.
Average amplitude (mV)			
Electrode size	40 mm	0.19	0.028
	56 mm	0.15	0.026
Average amplitude SD			
Electrode size	40 mm	0.074	0.028
	56 mm	0.048	0.011
ANOVA			
	F test	2.89	0.033
	p-value	0.103	0.857

that were produced by the 40 mm electrode setup have higher amplitude than the ones produced by the 56 mm electrode setup. This is an observation, that somewhat does imply that the size of the electrode has some impact on the resulting amplitude, but the differences in both R peak means and T wave maximum means between the two setups are small. When a one-way analysis of variance (ANOVA) is performed for the two to evaluate the statistical significance of these results, the results do not imply any. In Table 4.3, the ANOVA results are presented. For both R peak and T wave maximum the p-value calculated is greater than 0.05 usually used as the limit, meaning that it is not likely that the differences in the means are statistically significant.

Second evaluation point of view is the distance and overall placement of the electrodes. This comparison can be done between setups 1, 3 and 4, that have electrode distances of 5 cm, 15 cm, and 30 cm, respectively. While the electrodes in setup 1 are both on the left side of the chest, in setups 3 and 4 they are placed on both sides

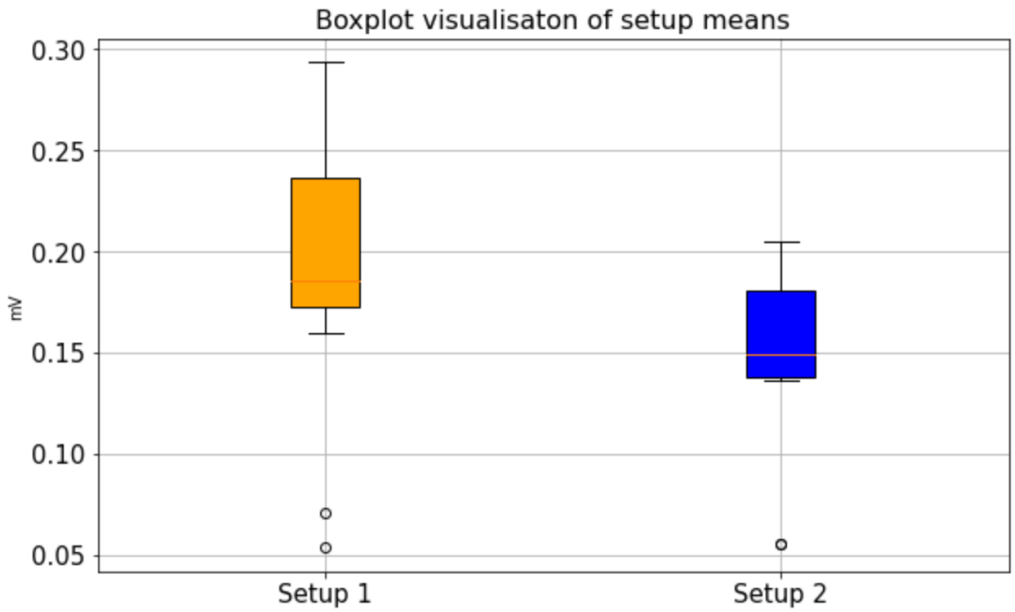

Figure 4.6: Boxplot visualisation of R peak means of the 40 mm electrode setup (setup 1) and the 56 mm electrode setup (setup 2). Both signals collected from the same subject.

of the sternum. Between all of the setups, setup 4 with 30 cm electrode distance had the highest average R peak amplitude. The largest difference in average waveforms in this comparison is between setups 1 and 4 (Figure 4.7). The average R peak amplitude for setup 1 is only 0.19 mV while it is over 0.73 mV in the signals produced by setup 4. Setup 3 falls between these two with average R peak amplitude at 0.24 mV.

With T waves, the highest average is again in the signals produced by the longest distance setup of 30 cm. Second highest average amplitude is setup 3 with 15 cm electrode distance, which is quite close to the average T wave maximum of the 30 cm distance setup with only 0.001 mV difference. Again the lowest average amplitude is produced by the 5 cm setup. The P wave is also more prominent in signals from the 30 cm setup. In the table below, the numeric comparison of R and T wave amplitudes from the above listed setups is found (Table 4.4). This comparison

implies that the R peak amplitude grows with the distance.

These differences, however, are so minor that it can be due to the small sample size. In the figure 4.7, the peaks are the other way around with the left chest setup producing higher average for R peak (Figure 4.7). This is due to individual differences. The boxplot visualisation of the R peak means of all three setups show that the 5 cm distance setup and the 15 cm distance setup have overlapping interquartile ranges (Figure 4.8), implicating statistically non-significant differences in the R peak amplitudes. This is further confirmed by ANOVA performed to compare the R peaks of the different setups. The results from the ANOVA are presented in the Table 4.4. The setup with 15 cm electrode distance has greater standard deviation, meaning that the individual differences have had a greater impact on the results.

Table 4.4: Average amplitudes of R and T waves and one way ANOVA results of R peak comparison of setups with electrode distances of 5, 15, and 30 cm.

Wave		R peak	T wave max.	S wave
Average amplitude (mV)				
Electrode distance	5 cm	0.19	0.028	-0.17
	15 cm	0.24	0.079	-0.25
	30 cm	0.73	0.080	-0.59
Average amplitude SD				
Electrode distance	5 cm	0.074	0.028	0.094
	15 cm	0.098	0.040	0.148
	30 cm	0.090	0.023	0.093
Comparison sets		5 & 15	5 & 30	15 & 30
ANOVA				
	F test	1.961	275.035	189.807
	p-value	0.174	<0.01	<0.01

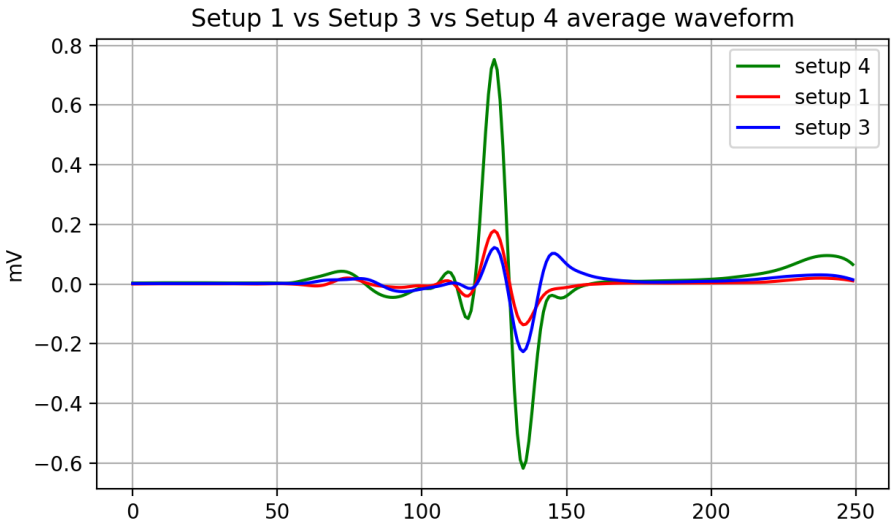

Figure 4.7: Visualisation of average waveforms of signals produced by setups 1, 3, and 4. All signals collected from the same subject.

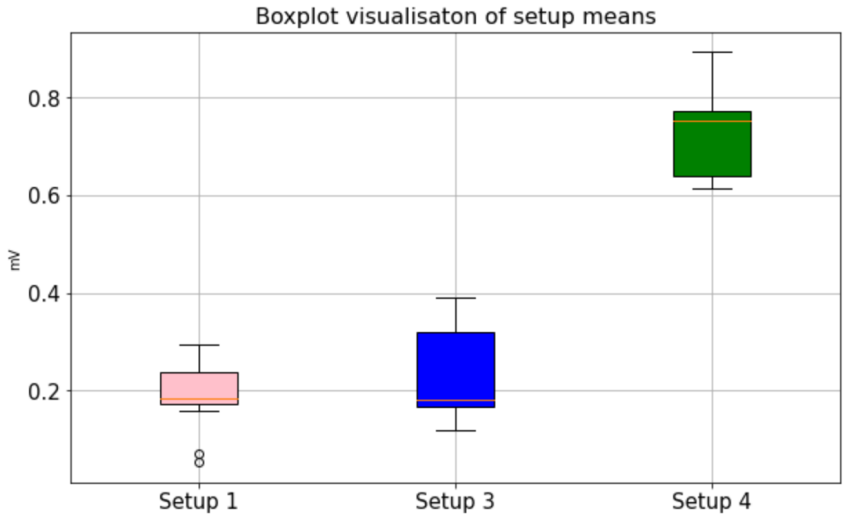

Figure 4.8: Boxplot visualisation of R-peak amplitude means of setups 1, 3, and 4.

In terms of quality, a somewhat important remark to be made is that the longer distance seems to produce more stable quality signals, according to the calculated PCC (Table 4.2).

The S an Q waves differ between setups 1 and 3, and 4 as well. In setup 1, the abso-

lute of the average S amplitude is only 11 % smaller than the average R amplitude, while in setup 3 the S wave is even deeper than the R peak is high. In average, setup 4 produces an S wave deeper than the R wave is high. In table 4.4, the average R and S waves from the three setups are compared. The deepest average S wave in relation to the R peak out of the three can be found in the setup 3.

The third and last observable feature of the devices was the electrode material. In this case, three different materials are compared: an Ag/AgCl wet electrode, conductive polymer electrode, and dry silver electrode. These were used in setups 3, 6, and 5, respectively. The exact material of the conductive polymer electrode is not known. Setup 3 was chosen for this comparison, as its electrode placement most closely resembles the electrode placement of the heart rate belt.

In this comparison, it is important to note that also the electrode distance varies greatly. The smallest difference in electrode distance is between setup 3 and the heart rate belt. The electrodes of both setups are circa 15 cm apart from each other on both sides of the sternum. In setup 3, the electrodes were placed above, and in setup 6, or the belt, below the breasts. Setup 5, or the necklace, was held between two fingers, which makes the electrode distance greater than either of the two before mentioned. It is, however, included, to compare the overall signal quality between the different materials.

In terms of amplitudes of the signals, the highest average R peak amplitude is produced by the HR belt. After the belt, the patch setup 3 produces the second highest R peak average. The necklace has the lowest R peak average amplitude of the three. This might be highly affected by the poor signal quality of the necklace setup. When it comes to the T waves, the order is slightly different, with the setup 3 producing the highest T wave average maximum. The necklace setup has again the lowest average amplitude of T wave, but the wave itself was completely missing or unclear in multiple measurements leaving room for error. The comparison of the average amplitudes of R and T waves is displayed in table 4.5 as well. At least for the R peak differences, the ANOVA results imply statistical significance between all setups (Table 4.5).

Table 4.5: Average amplitudes of R and T waves and one way ANOVA results of R peak comparison of setups with different electrode materials.

Wave		R peak	T wave max.	S wave
Average amplitude (mV)				
Electrode material	Ag/AgCl	0.24	0.079	-0.25
	Silver	0.13	0.024	-0.075
	Plastic polymer	0.53	0.059	-0.43
Average amplitude SD				
Electrode material	Ag/AgCl	0.098	0.040	0.148
	Silver	0.063	0.017	0.090
	Plastic polymer	0.164	0.026	0.144
Comparison sets		Ag/AgCl & Silver	Ag/AgCl & Polymer	Silver & Polymer
R peak ANOVA				
	F test	9.374	31.162	56.188
	p-value	<0.01	<0.01	<0.01

When it comes to the signal quality and stability, the best way to look into that is the correlation of the PQRST waveforms to the waveform average. From the electrode material point of view, the Ag/AgCl wet electrode setup produces the best correlative waveforms when compared to the reference signal. The smallest correlation is calculated for the necklace setup, or the dry silver electrode. The conductive polymer electrode produces similar quality signal to the reference device. The same Ag/AgCl wet electrodes were used in both setup 3 and the reference device. The comparison is displayed in table 4.6.

Table 4.6: Average Pearson correlation coefficients of PQRST-waveforms of setups 3, 5, and 6. In the last column, the difference between DUT and reference signal correlation in percentages.

Setup	Electrode material	Average PCC of DUT	Average PCC of Reference	Difference in %
3	Ag/AgCl	0.9943	0.9660	+3
5	Silver	0.8064	0.9560	-16
6	Conductive polymer	0.9559	0.9515	+0.005

In the figures 4.9 and 4.10, the waveform average of a single measurement produced by the setups with dry electrodes are compared to the same signal produced by the setup with the traditional wet electrodes. When comparing the setups 3 and 5, the waveforms have great differences. The waveform average of signal 5 seems to have no Q-wave present and both the P-wave and the T-wave are nearly invisible, while setup 3 seems to produce clear waves.

The differences between the wet electrode setup 3 and the heart rate belt are smaller, but still visible. The average waveform calculated from the signal produced by the belt setup has all the waves present, but they are slightly clearer than the ones produced by the wet electrode setup 3. In the example waveform visible in figure 4.10, the S-wave from the belt setup returns to the baseline slower than the S-wave of the setup 3.

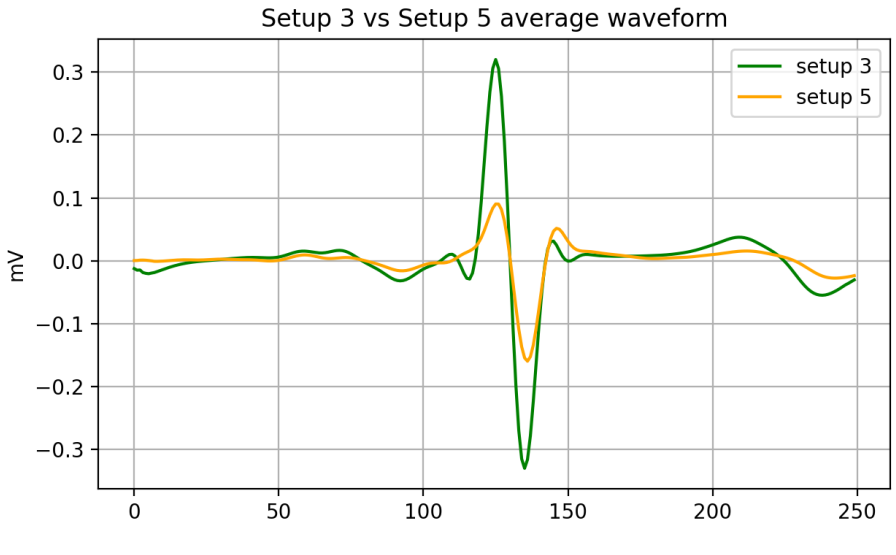

Figure 4.9: Visualisation of average waveforms of signals produced by setups 3 (wet electrode) and 5 (necklace). Both signals collected from the same subject.

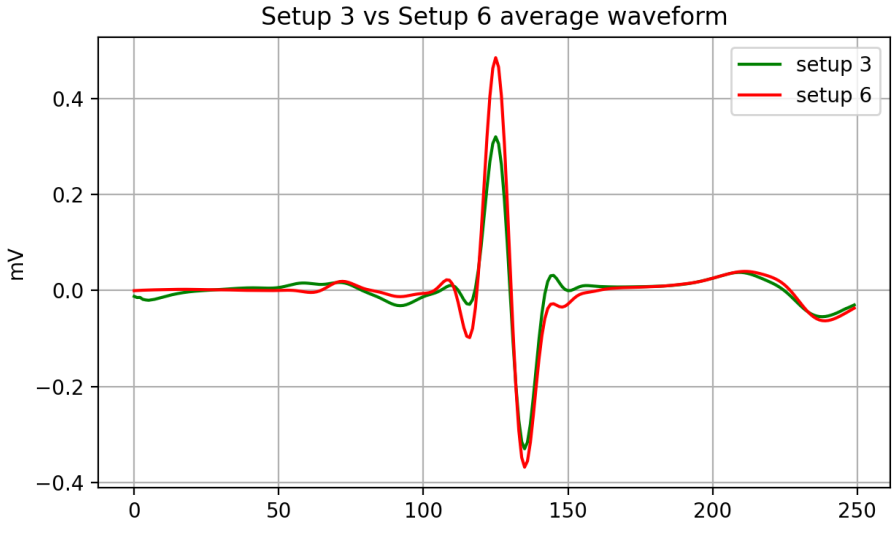

Figure 4.10: Visualisation of average waveforms of signals produced by setups 3 (wet electrode) and 6 (heart rate belt). Both signals collected from the same subject.

Comparing the height of the R-wave versus the depth of the S-wave, the necklace setup has, in average, lowest S-wave amplitude absolute compared to the R-wave absolute amplitude (Table 4.5). The signals produced by the wet electrode setup 3 and the belt have higher S-wave averages compared to R-peak. The belt also produces an S-wave average absolute amplitude lower than that of R peak while the wet electrode setup 3, in average, has deeper S-wave than R-peaks are high. The averages are calculated from all the measurements taken with the same setup, so individual differences can occur.

4.2 The Results in Comparison With the Previous Research

With the first comparison, the electrode size was considered. In 2020, Nairn (et al), concluded that increasing the size of the electrode has a negative impact on the amplitude of an electogram (Nairn et al. 2020). The measurement results of this experiment do imply a similar effect. When looking into the average waveforms, the higher average peaks are produced by the setups with the smaller electrodes. The ANOVA, however, does not support this conclusion. In this case, it would be important to gather more data to better evaluate the differences. The electrode size is a factor that can affect, for example, the hospital bedside monitoring devices as well as ambulatory diagnostic devices since they usually have some kind of clip-in electrodes such as the Ambu ones used in this experiment (Ambu 2021a, Ambu 2021b).

When it comes to the electrode distance, the best reference is the differences between the leads. As they are standardised, they already take into account how the

positioning affects the signal waveform. For example, the Mason-Likar modification has been proven to affect the signal amplitudes differently depending on the leads (Rautaharju et al. 1980). This feature was and is difficult to evaluate with the setups chosen for this experiment. Looking purely at the average R peaks, it seems that the results stand somewhat in line with the ones presented by Rautaharju (et al) in 1980, as the attempted mimicking of lead I seems to cause the R peaks to have higher amplitudes with greater distance. When taking into account the ANOVA results, the results from this experiment remain inconclusive between the 5 cm setup and 15 cm setup. The 30 cm setup differs statistically from the shorter distance setups, but the overall electrode placement might affect the final results as well.

In wearable devices, however, the electrode placement is not standardised as it is in the 12-lead diagnostic ECG. This is why the use case of each setup should be considered when evaluating their usability and quality. In this case, it is visible that longer distance between electrodes, with these specific electrode placements, give, for example, more prominent R peaks. With clear R peaks and high quality signal, evaluating the rhythm is possible and the higher the R peaks, the easier it is to automatically detect them. In this experiment, the wet electrode setups were mimicking a patch type setup, except for the 30 cm distance setup. The patch type setup has already been recognised as a valid tool to observe the rhythm (Murali et al. 2020). This experiment further validates those results with the signals produced having clean and consistent waveforms, from which the rhythm can be calculated.

Comparing the electrode materials, the polymer electrode resembles most a textile electrode studied by Nigusse (et al). The study suggests, that the textile electrodes are better suited for longer measurements as they do not dry like the single-use wet electrodes and thus create disruptancies in the signal due to poor skin contact (Nigusse et al. 2021). This experiment does not contradict that conclusion, as

the correlation of waveforms to the waveform average between the similarly placed electrodes is quite near each other, implying stable skin contact and thus signal quality. It is however notable, that the traditional wet electrode produces a slightly more stable signal in terms of quality. An observation that is longer than only 60 seconds (used in this experiment) might give different results. All in all, it can be stated that the quality is not notably worse in either of the setups.

The dry silver electrode in the necklace, on the other hand, shows poor overall signal quality. It has been stated that these types of dry electrodes are sensitive to contact issues (Meziane et al. 2013), which are suspected to have the biggest effect on the signal in this experiment as well. The necklace was the only device that had to be held in place by hand, leading to possible movement and connection breakages during the measurements. In this case, it can be stated that the results are in line with previous studies.

4.3 Limitations of the Experiment

The way that the signals were collected has some limitations. The main issues are with signal quality and synchronisation of the reference signal with the observable devices' signal. Due to the devices being connected to different power sources and the signal recordings being done separately, the start time of the recordings can differ.

The differences in starting time might further lead to differing duration of the measurements. This can cause, for example, the number of peaks to be greater in the observable signal. At most, we are seeing one to two seconds difference. This can be mitigated by cropping the signals to shorter duration.

The two signals have also differing sampling rates. The sampling rate of the reference signal is 100 Hz while it is 128 Hz in the observable signal. The signals were resampled to match.

Due to some lag in the GE Patient monitor recordings, the signal in the recording only starts after one second of the record's start. This was observed to be a feature of the device. It is mitigated in the analysis phase by cropping the data to start only after 150 samples, which is 1.5 seconds.

In addition, the dataset collected for this experiment is quite small. It would be easier to see trends or clearer differences between the setups from a larger dataset. For the purpose of this thesis, the size of the dataset is adequate.

When it comes to selected features, the measurements could have been conducted with different electrode placements to get better comparability. For example, the setups with the wet electrodes (1, 3, and 4) had too different placements to accurately evaluate the effect of electrode distance on the selected waveform features. The ideal placement for small, wearable devices was difficult to determine, as even the slightest adjustment can have an effect on the waveform, as explained in the theory on the ECG leads. One possible countermeasure would be to mark the electrode placements with a marker and measure the distances with a ruler or measuring tape.

4.4 Future Research Possibilities

As the wearable devices are still a growing trend, these topics could be revisited with a larger dataset and more specific research questions. For example, it would be interesting and useful to explore the signal quality further with more focus on the frequency domain changes. Additionally, a deeper dive into the basic problems

that the wearable devices should solve would be beneficial. The use cases for single lead ECG devices are not too numerous so exploring the possibilities is still valid. For example, observing how the electrode distance affects the long term usability of a wearable setup could be one approach.

In this experiment, the measurements were taken from presumably healthy individuals. Another possibility would be to inspect certain known ECG abnormalities with similar protocol. One example could be observing the premature ventricular contractions (PVCs) in the single-lead setups, as they are among the most common arrhythmias (Mäkijärvi and Aro 2019). This would give a better image of the true possibilities and limitations of these type of devices.

Moreover, a full 12-lead ECG comparison to find the ideal electrode placements for observing, for example, specific heart conditions could provide more information on the wearable devices and how they can be used. As this experiment only had one comparison lead, the full 12-lead system as reference would provide more important information to optimise the single lead placements since they are not yet standardised.

5 Conclusions

From the literature referenced in this thesis, the conclusion is that the single lead ECG devices cannot replace the standard 12 lead ECG anytime soon. The three-dimensionality of the human heart makes it impossible to reliably observe all sides from only one lead, which can lead to misdiagnosis or completely missing the diagnosis.

Whether or not the single lead ECG can be deemed reliable, depends on the use case: in rhythm tracking, the literature supports the use of single lead devices in monitoring. The experiment conducted for this thesis supports the conclusion that the overall signal quality in these types of measurement setups is good.

The question of the electrodes, on the other hand, gives more information on the possibilities. The electrode material and design, as observed in the experiment, has the greatest effect on the signal quality. The traditional wet electrodes give more stable results than the dry electrodes.

Electrode placement affects the signal as well. Most of the differences can be traced back to the bioelectrical phenomena in the heart and how the different placements pick up the signal. The distance, in this experiment, does not show statistically significant effect on the amplitudes of the waves for the most part. The research by Rautaharju et al. 1980, however, supports the hypothesis that the distance of the

electrodes do have an impact on the resulting signal and this impact depends highly on the lead measured.

Lastly, the electrode size is also observed to have an effect on the resulting signal, while this experiment does not prove it to be statistically significant. However, this result and conclusion are in line with the previous research as well. These differences are small in both the reference literature and this experiment.

In total, the different features and setups explored in the experiment phase of this thesis give a broad picture of the effects that changes in the measurement protocols have in the resulting signal quality and waveform wise.

References

Adamec, Jan and Richard Adamec (2008). "Technical Aspects". In: *ECG Holter: Guide to Electrocardiographic Interpretation*. Boston, MA: Springer US, pp. 1–8. ISBN: 978-0-387-78187-7. DOI: 10.1007/978-0-387-78187-7_1. URL: https://doi.org/10.1007/978-0-387-78187-7_1.

AlGhatrif, Majd and Joseph Lindsay (2012). "A brief review: history to understand fundamentals of electrocardiography". In: *Journal of community hospital internal medicine perspectives* 2.1, p. 14383.

Ambu (2021a). *BlueSensor M*. URL: https://www.ambu.com/Admin/Public/DWSDownload.aspx?File=%2fFiles%2fFiles%2fDownloads%2fAmbu+com%2fCardiology%2fShort-term_ECG_monitoring_electrodes%2fBlueSensor+M%2fDatasheets%2fLBL-007445-M-Datasheet_IE_V01_202110_TCC-11108.pdf.

— (2021b). *BlueSensor R*. URL: https://www.ambu.com/Admin/Public/DWSDownload.aspx?File=%2fFiles%2fFiles%2fDownloads%2fAmbu+com%2fCardiology%2fStress_ECG_electrodes%2fBlueSensor+R%2fDatasheets%2fLBL-007450_R-Datasheet_IE_V01_202110_TCC-11109.pdf.

An, Xiang and George K. Stylios (2018). "A Hybrid Textile Electrode for Electrocardiogram (ECG) Measurement and Motion Tracking". In: *Materials* 11.10. ISSN: 1996-1944. URL: https://www.mdpi.com/1996-1944/11/10/1887.

Barold, Serge S (2003). "Willem Einthoven and the birth of clinical electrocardiography a hundred years ago". In: *Card Electrophysiol Rev.* DOI: 10.1023/a:1023667812925. URL: https://pubmed.ncbi.nlm.nih.gov/12766530/.

Birnbaum, Yochai, James M. Wilson, and Kjell Nikus (2015). "The Electrocardiogram in Coronary Artery Disease". In: *Coronary Artery Disease*. Ed. by James T. Willerson and David R. Holmes Jr. London: Springer London, pp. 205–216. ISBN: 978-1-4471-2828-1. DOI: 10.1007/978-1-4471-2828-1_9. URL: https://doi.org/10.1007/978-1-4471-2828-1_9.

Bortolan, Giovanni et al. (2015). "Noise processing in exercise ECG stress test for the analysis and the clinical characterization of QRS and T wave alternans". In: *Biomedical Signal Processing and Control* 18, pp. 378–385.

Duodecim (2021). *Eteisvärinä*. Ed. by Suomalaisen Lääkäriseuran Duodecimin ja Suomen Kardiologisen Seuran asettama työryhmä. URL: www.kaypahoito.fi.

Eerola, Hannaleena (2022). "EKG (sydänfilmi)". In: *Osoitteessa: https://www.terveyskirjasto.fi/*

Fontana, Piero et al. (2019). "Clinical Applicability of a Textile 1-Lead ECG Device for Overnight Monitoring". In: *Sensors* 19.11. ISSN: 1424-8220. DOI: 10.3390/s19112436. URL: https://www.mdpi.com/1424-8220/19/11/2436.

Goldberger, Ary L., Zachary D. Goldberger, and Alexei Shvilkin (2018a). "Chapter 3 - How to Make Basic ECG Measurements". In: *Goldberger's Clinical Electrocardiography (Ninth Edition)*. Ed. by Ary L. Goldberger, Zachary D. Goldberger, and Alexei Shvilkin. Ninth Edition. Elsevier, pp. 11–20. ISBN: 978-0-323-40169-2. DOI: https://doi.org/10.1016/B978-0-323-40169-2.00003-2. URL: https://www.sciencedirect.com/science/article/pii/B9780323401692000032.

— (2018b). "Chapter 4 - ECG Leads". In: *Goldberger's Clinical Electrocardiography (Ninth Edition)*. Ed. by Ary L. Goldberger, Zachary D. Goldberger, and Alexei Shvilkin. Ninth Edition. Elsevier, pp. 21–31. ISBN: 978-0-323-40169-2. DOI:

https://doi.org/10.1016/B978-0-323-40169-2.00004-4. URL: https://www.sciencedirect.com/science/article/pii/B9780323401692000044.

Haverkamp, Haakon Tillmann, Stig Ove Fosse, and Peter Schuster (2019). "Accuracy and usability of single-lead ECG from smartphones-A clinical study". In: *Indian pacing and electrophysiology journal* 19.4, pp. 145–149.

He, Runnan et al. (2018). "Automatic Detection of Atrial Fibrillation Based on Continuous Wavelet Transform and 2D Convolutional Neural Networks". In: *Frontiers in Physiology* 9. ISSN: 1664-042X. DOI: 10.3389/fphys.2018.01206. URL: https://www.frontiersin.org/articles/10.3389/fphys.2018.01206.

Hilbel, Thomas and Norbert Frey (2023). "Review of current ECG consumer electronics (pros and cons)". In: *Journal of Electrocardiology* 77, pp. 23–28.

Korhonen, Petri and Markku Mäkijärvi (2019). *EKG*. fin. Ed. by Markku Mäkijärvi et al. Tarkistettu ja päivitetty versio. Article reference ekg00005. Helsinki: Kustannus Oy Duodecim. ISBN: 978-952-360-057-7.

Kossmann, Charles E. and Franklin D. Johnston (1935). "The precordial electrocardiogram: I. The potential variations of the precordium and of the extremities in normal subjects". In: *American Heart Journal* 10.7, pp. 925–941. ISSN: 0002-8703. DOI: https://doi.org/10.1016/S0002-8703(35)90422-7. URL: https://www.sciencedirect.com/science/article/pii/S0002870335904227.

Laukkanen, Jari and Tuomo Nieminen (2016). *Kardiologia*. eng. Ed. by Juhani Airaksinen et al. Uudistettu [versio]. Article reference kar01417. Helsinki: Kustannus Oy Duodecim. ISBN: 978-951-656-600-2.

Lee, Stephen and John Kruse (2008). "Biopotential electrode sensors in ECG/EEG/EMG systems". In: *Analog Devices* 200, pp. 1–2.

Lobodzinski, S. Suave (2013). "ECG Patch Monitors for Assessment of Cardiac Rhythm Abnormalities". In: *Progress in Cardiovascular Diseases* 56.2. Ambulatory ECG Monitoring: Clinical Practice and Research Applications, pp. 224–

229. ISSN: 0033-0620. DOI: https://doi.org/10.1016/j.pcad.2013.08.006. URL: https://www.sciencedirect.com/science/article/pii/S0033062013001515.

Mäkijärvi, Markku (2019a). *EKG*. fin. Ed. by Markku Mäkijärvi et al. Tarkistettu ja päivitetty versio. Article reference ekg00001. Helsinki: Kustannus Oy Duodecim. ISBN: 978-952-360-057-7.

— (2019b). *EKG*. fin. Ed. by Markku Mäkijärvi et al. Tarkistettu ja päivitetty versio. Article reference ekg00010. Helsinki: Kustannus Oy Duodecim. ISBN: 978-952-360-057-7.

Mäkijärvi, Markku and Aapo Aro (2019). *EKG*. fin. Ed. by Markku Mäkijärvi et al. Tarkistettu ja päivitetty versio. Article reference ekg00075. Helsinki: Kustannus Oy Duodecim. ISBN: 978-952-360-057-7.

Mäkijärvi, Markku and Petri Korhonen (2019). "EKG-kytkennät". In: *EKG*. Kustannus Oy Duodecim. ISBN: 9516560938.

Mason, Robert E and Ivan Likar (1966). "A new system of multiple-lead exercise electrocardiography". In: *American heart journal* 71.2, pp. 196–205.

Meziane, N et al. (2013). "Dry electrodes for electrocardiography". In: *Physiological measurement* 34.9, R47.

Movesense (2023a). *API Reference*. URL: https://www.movesense.com/docs/esw/api_reference/.

— (2023b). *Best Practices*. URL: https://www.movesense.com/docs/system/best_practices/.

— (2023c). *Hardware Variants*. URL: https://www.movesense.com/docs/system/hw_variants/.

Murali, Srinivasan et al. (2020). "Cardiac ambulatory monitoring: new wireless device validated against conventional Holter monitoring in a case series". In: *Frontiers in Cardiovascular Medicine* 7, p. 587945.

Nairn, Deborah et al. (2020). "Impact of electrode size on electrogram voltage in healthy and diseased tissue". In: *2020 Computing in Cardiology*. IEEE, pp. 1–4.

Nault, Isabelle et al. (2019). "Validation of a novel single lead ambulatory ECG monitor – Cardiostat™ – Compared to a standard ECG Holter monitoring". In: *Journal of Electrocardiology* 53, pp. 57–63. ISSN: 0022-0736. DOI: https://doi.org/10.1016/j.jelectrocard.2018.12.011. URL: https://www.sciencedirect.com/science/article/pii/S0022073618305673.

Nigusse, Abreha Bayrau et al. (2021). "Wearable Smart Textiles for Long-Term Electrocardiography Monitoring—A Review". In: *Sensors* 21.12. ISSN: 1424-8220. URL: https://www.mdpi.com/1424-8220/21/12/4174.

Nikus, Kjell, Aapo Aro, and Markku Mäkijärvi (2016). *Kardiologia*. eng. Ed. by Juhani Airaksinen et al. Uudistettu [versio]. Article reference kak01143. Helsinki: Kustannus Oy Duodecim. ISBN: 978-951-656-600-2.

Oy, Polar Electro (2020). *Polar H1 HR sensor*. URL: https://www.polar.com/fi/sensors/h10-heart-rate-sensor.

Oy, Suunto (2020). *Suunto Smart HR Belt*. URL: https://www.suunto.com/fi-fi/Tuotteet/Sykevyot/suunto-smart--sykevyo/.

Piwek, Lukasz et al. (2016). "The rise of consumer health wearables: promises and barriers". In: *PLoS medicine* 13.2, e1001953.

Raatikainen, Pekka, Markku Mäkijärvi, and Hannu Parikka (2019a). *EKG*. fin. Ed. by Markku Mäkijärvi et al. Tarkistettu ja päivitetty versio. Article reference ekg00175. Helsinki: Kustannus Oy Duodecim. ISBN: 978-952-360-057-7.

— (2019b). *EKG*. fin. Ed. by Markku Mäkijärvi et al. Tarkistettu ja päivitetty versio. Article reference ekg00176. Helsinki: Kustannus Oy Duodecim. ISBN: 978-952-360-057-7.

Raatikainen, Pekka and Hannu Parikka (2017). "EKG: n tulkinta aikuisilla". In: *Lääkärin käsikirja*. Duodecim, pp. 158–161.

Rautaharju, PM et al. (1980). "The effect of modified limb electrode positions on electrocardiographic wave amplitudes". In: *Journal of electrocardiology* 13.2, pp. 109–113.

Rauttola, Ari-Pekka et al. (2019). *Puettavan teknologian hyödyntäminen työterveyshuolloissa ja työpaikoilla.*

Santala, Onni Elmeri (2022). "Novel ECG-based technologies in the detection of atrial fibrillation". PhD thesis. Itä-Suomen yliopisto.

SciPy, Community (2023a). *scipy.signal.resample*. URL: https://docs.scipy.org/doc/scipy/reference/generated/scipy.signal.resample.html.

— (2023b). *scipy.signal.sosfiltfilt*. URL: https://docs.scipy.org/doc/scipy/reference/generated/scipy.signal.sosfiltfilt.html.

— (2023c). *scipy.signal.welch*. URL: https://docs.scipy.org/doc/scipy/reference/generated/scipy.signal.welch.html.

Statista (Jan. 2024). *Wearable device usage 2023*. URL: https://www.statista.com/forecasts/1101110/wearables-devices-usage-in-selected-countries.

Steinberg, Jonathan S et al. (2017). "2017 ISHNE-HRS expert consensus statement on ambulatory ECG and external cardiac monitoring/telemetry". eng. In: *Heart rhythm* 14.7, e55–e96. ISSN: 1547-5271.

Steinhubl, Steven R. et al. (July 2018). "Effect of a Home-Based Wearable Continuous ECG Monitoring Patch on Detection of Undiagnosed Atrial Fibrillation: The mSToPS Randomized Clinical Trial". In: *JAMA* 320.2, pp. 146–155. ISSN: 0098-7484. DOI: 10.1001/jama.2018.8102. eprint: https://jamanetwork.com/journals/jama/articlepdf/2687353/jama_steinhubl_2018_oi_180066.pdf. URL: https://doi.org/10.1001/jama.2018.8102.

Swant, Marty (2020). *The 2020 world's most valuable brands*. URL: https://www.forbes.com/the-worlds-most-valuable-brands/.

Thaler, Malcolm (2018a). "The 12 views of the Heart". In: *The Only EKG Book You'll Ever Need*. Lippincott Williams & Wilkins, pp. 55–66.

— (2018b). "The 12 views of the Heart". In: *The Only EKG Book You'll Ever Need*. Lippincott Williams & Wilkins, pp. 69–81.

— (2018c). *The only EKG book you'll ever need*. Lippincott Williams & Wilkins, pp. 31–42.

Using Apple Watch for Arrhythmia Detection (Dec. 2020). URL: https://www.apple.com/healthcare/docs/site/Apple_Watch_Arrhythmia_Detection.pdf.

SinusRhythmLabels.svg (2007). URL: https://commons.wikimedia.org/wiki/File:SinusRhythmLabels.svg.

Yang, Xiang-Lin et al. (2015). "The history, hotspots, and trends of electrocardiogram". In: *Journal of geriatric cardiology: JGC* 12.4, p. 448.